Biol. Cybern. 70, 359–368 (1994)

Biological Cybernetics

Reduced-system analysis of the effects of serotonin on a molluscan burster neuron

Richard Bertram *

Department of Mathematics and Supercomputer Computations Research Institute, Florida State University, Tallahassee, FL 32306, USA

Received: 24 March 1993/Accepted in revised form: 9 June 1993

Abstract. The mathematical model described in Bertram (1993) is used to carry out a detailed examination of the manner in which the neurotransmitter serotonin modifies the voltage waveform generated endogenously by burster neuron R_{15} of *Aplysia*. This analysis makes use of a reduced system of equations, taking advantage of the slow rate of change of a pair of system variables relative to the others. Such analysis also yields information concerning the sensitivity of the neuron to brief synaptic perturbations.

1 Introduction

Neuron R_{15}, located in the abdominal ganglion of the marine mollusc *Aplysia*, is one well-known member of a class of cells known as *burster cells*. Other examples include the neurons L_2–L_6, also located in the *Aplysia* abdominal ganglion (Kramer and Zucker 1985a,b), several neurons from the parietal ganglion of *Helix* (Eckert and Lux 1976), and insulin-secreting β-cells found in the pancreas (Atwater et al. 1980). Some burster cells, such as pancreatic β-cells, typically burst only when coupled with other cells (Rorsman and Trube 1986). Others, including neuron R_{15}, generate a bursting voltage oscillation endogenously. This oscillation is periodic, each period consisting of a burst of voltage spikes followed by a quiescent interburst during which membrane potential is hyperpolarized and changes slowly.

A mathematical model of the bursting in R_{15} is described in Bertram (1993). This model, consisting of ten coupled nonlinear ordinary differential equations, incorporates all the major ionic currents known to exist in the axon hillock region of the neuron and generates a bursting voltage waveform with all the features of the actual waveform. Unlike earlier models (Plant and Kim 1975; Plant 1978), the present model includes the ionic mechanisms now thought to drive the bursting in the neuron and differs from the recent model of Canavier et al. (1991) primarily in the treatment of the two subthreshold "burst" currents.

* *Present address:* Mathematical Research Branch, NIDDK, NIH, Bethesda, MD 20892, USA

Laboratory studies (Drummond et al. 1980; Levitan and Levitan 1988) have shown that exogenous application of serotonin (5-hydroxytryptamine or 5-HT) to R_{15} results in major changes in the voltage waveform. Depending upon the concentration of 5-HT applied, the bursting may be enhanced, terminated, or transformed into a beating oscillation in which the neuron spikes tonically. The effects of 5-HT last for several hours.

The application of 5-HT to R_{15} was modeled in Bertram (1993), where it was found that besides the effects of 5-HT on the voltage waveform described above, 5-HT alters the sensitivity of the neuron to synaptic perturbations. In the present paper, a reduced system of equations which makes use of the slow rate of change of two system variables is used to analyze first the control bursting oscillation (i.e. no 5-HT), then the way in which 5-HT modifies this oscillation, and finally the effects of voltage perturbations applied to the system under the influence of various concentrations of 5-HT.

2 Mathematical models

2.1 The R_{15} model

We give here a brief account of the mathematical model of R_{15} which is described in detail in Bertram (1993). The model incorporates eight ionic currents, yielding a system of ten differential equations. Of these currents, five are *spike* currents and three are *subthreshold* currents. The former generate the action potentials while the latter are responsible for driving the bursting oscillation. The equation describing the rate of change of membrane potential is

$$\frac{dV}{dt} = -(I_{spike} + I_{sub} - I_{app})/C_M \tag{1}$$

where

$$I_{spike} = I_{Na} + I_{Ca} + I_{K1} + I_{K2} + I_L \tag{2}$$

$$I_{sub} = I_{NSR} + I_D + I_R \tag{3}$$

and C_M is the membrane capacitance. I_{Na} and I_{Ca} are excitatory sodium and calcium currents, while I_{K1} and

I_{K2} are inhibitory potassium currents. I_L is a small leakage current and the applied current, I_{app}, is set to zero in the discussions which follow.

The bursting oscillation is generated by the interaction of the two subthreshold excitatory currents I_{NSR} and I_D. I_{NSR} is a calcium current which initiates the burst and then inactivates during the burst as calcium ions accumulate inside the cell. I_D is a cation-nonspecific current which summates during the burst. When the sum of these two current falls below threshold the burst terminates and membrane potential falls to a hyperpolarized value following a voltage excursion known as the depolarizing after-potential (DAP). The model bursting oscillation is shown in Fig. 1.

The equations used to describe I_{NSR} and I_D are

$$I_{NSR} = \bar{g}_{NSR} q^4 y_\infty(V)(V - V_{Ca}) \tag{4}$$

$$I_D = -z \tag{5}$$

where

$$\frac{dq}{dt} = [q_\infty(c) - q]/\tau_q(V) \tag{6}$$

$$\frac{dz}{dt} = k_z m^3 h - z/\tau_z. \tag{7}$$

The maximal conductance of I_{NSR} is denoted by $\bar{g}_{NSR}$, while V_{Ca} is the calcium equilibrium potential. The factor $y_\infty(V)$ represents steady-state activation, while q is a calcium-dependent inactivation variable. The variable c denotes intracellular free calcium concentration and the function $\tau_q(V)$ is large compared to the time constant of most other variables, ensuring that q will approach its equilibrium value q_∞ slowly. The term $k_z m^3 h$ in (7) ensures that I_D increases with each spike, while $-z/\tau_z$ ensures that the current decays exponentially between spikes. The constant τ_z is large, so that z will change slowly between spikes and between bursts of spikes.

2.2 Simulated application of serotonin

When 5-HT is applied exogenously to R_{15} at least two things happen: the maximal conductance of I_{NSR} is increased, and the maximal conductance of the subthreshold *inward rectifier* (I_R) is increased (Drummond et al. 1980; Benson and Levitan 1983; Lotshaw et al. 1986; Levitan and Levitan 1988). In the present model, the latter current is given by

$$I_R = \bar{g}_R r_\infty(V)(V - V_K) \tag{8}$$

where $\bar{g}_R$ is the maximal conductance and $r_\infty(V)$ is the steady-state activation function. I_R is a potassium current which is activated only at voltages near the potassium equilibrium potential V_K. In the absence of 5-HT, the outward current generated by I_R is so small that it plays no significant role in the generation of the bursting oscillation. However, in the presence of 5-HT this current becomes significant.

Application of 5-HT was first simulated in Canavier et al. (1991) by varying the maximal conductance of an inward-rectifying potassium current and, for large 5-HT concentrations, the conductance of a slowly inactivating current similar to I_{NSR}. In Bertram (1993) the application of 5-HT was modeled by defining a functional relationship between the maximal conductance of I_R and I_{NSR} and a dimensionless parameter S, which is a measure of serotonin concentration. The currents then become

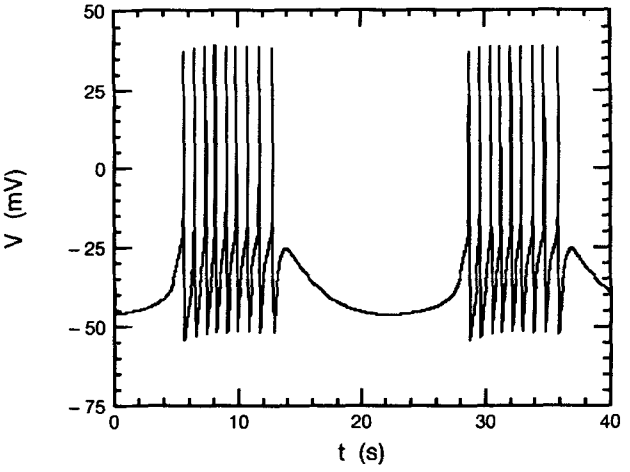

Fig. 1. Model bursting oscillation. The DAP, or voltage "hump" following each burst of spikes, is a common feature of the R_{15} oscillation

$$I_{NSR} = \bar{G}_{NSR} q^4 y_\infty(V)(V - V_{Ca}) \tag{9}$$

$$I_R = \bar{G}_R r_\infty(V)(V - V_K) \tag{10}$$

where $\bar{G}_{NSR}(S)$ and $\bar{G}_R(S)$ are functions defined for $S \in [0, 1]$ having the following properties:

1. $\bar{G}_{NSR}(0) \approx \bar{g}_{NSR}$, $\bar{G}_R(0) \approx \bar{g}_R$
2. Both $\bar{G}_{NSR}$ and $\bar{G}_R$ are saturated at $S = 1$
3. $\bar{G}_{NSR}$ and $\bar{G}_R$ are sigmoidal
4. $\bar{G}_R$ increases and saturates earlier than $\bar{G}_{NSR}$

Expressions for these functions are given in Bertram (1993).

2.3 The reduced R_{15} model

Since variables z and q change slowly compared with other variables in the R_{15} model, it is helpful to examine the asymptotic solution structure of a reduced system of equations, where z and q are treated as parameters. The entire bursting oscillation can then be constructed from the reduced system by slowly varying these two parameters. A similar approach has proven sucessful in several earlier studies of bursting oscillations (Chay and Rinzel 1985; Rinzel and Lee 1987; Decroly and Goldbeter 1987; Canavier et al. 1991).

The full system may be expressed formally in vector form as

$$\frac{d}{dt}\vec{\mathbf{U}} = \vec{\mathbf{F}}(\vec{\mathbf{U}}; S) \tag{11}$$

where $\vec{U}$ is a ten-dimensional vector and $\vec{F}$ is a ten-dimensional vector function. The role played by S as the single system parameter subject to variation is highlighted. Following a similar formalism, the reduced system may be expressed as

$$\frac{d}{dt}\vec{V} = \vec{G}(\vec{V}; S, z, q) \tag{12}$$

where $\vec{V}$ and $\vec{G}$ are now eight-dimensional and z and q are additional parameters. The complete set of equations is included in the Appendix.

3 Analysis of the modulated voltage waveform

3.1 Dissection of the control bursting oscillation

Each period of the bursting oscillation consists of an active phase of spiking followed by a passive phase of slow voltage variation. Intuitively, this corresponds to passage from a periodic "spiking" attractor to a stationary attractor as the two "slow" parameters z and q are varied. The control ($S = 0$) bursting oscillation generated by (11) is dissected in Fig. 2. Immediately prior to the first spike of the burst, $z \approx 0.045$ nA $\approx z_\infty$ (where $z_\infty = \tau_z k_z m_\infty^3 h_\infty$). For this value of z the stable and unstable solution branches of the reduced system (12) are traced out in Fig. 2a, using q as the bifurcation parameter. The stationary branches are constructed using the automatic branch continuation and bifurcation program AUTO (Doedel 1981). The periodic spiking branch is constructed using a combination of AUTO and direct numerical integration of (12).

Superimposed on this bifurcation diagram is the projection onto the $q - V$ phase plane of the first spike generated by (11). From location A the orbit moves to the right along the lower reduced-system stable stationary branch (labeled $N^S_{0,0.045}$) as q approaches its equilibrium value, $q_\infty = 1/(1 + 2c_\infty)$. Since no stable equilibrium solution to (11) exists for $S = 0$, $N^S_{0,0.045}$ terminates before q_∞ is reached. Thus, there is a saddle-node bifurcation located at $q < q_\infty$ in which the

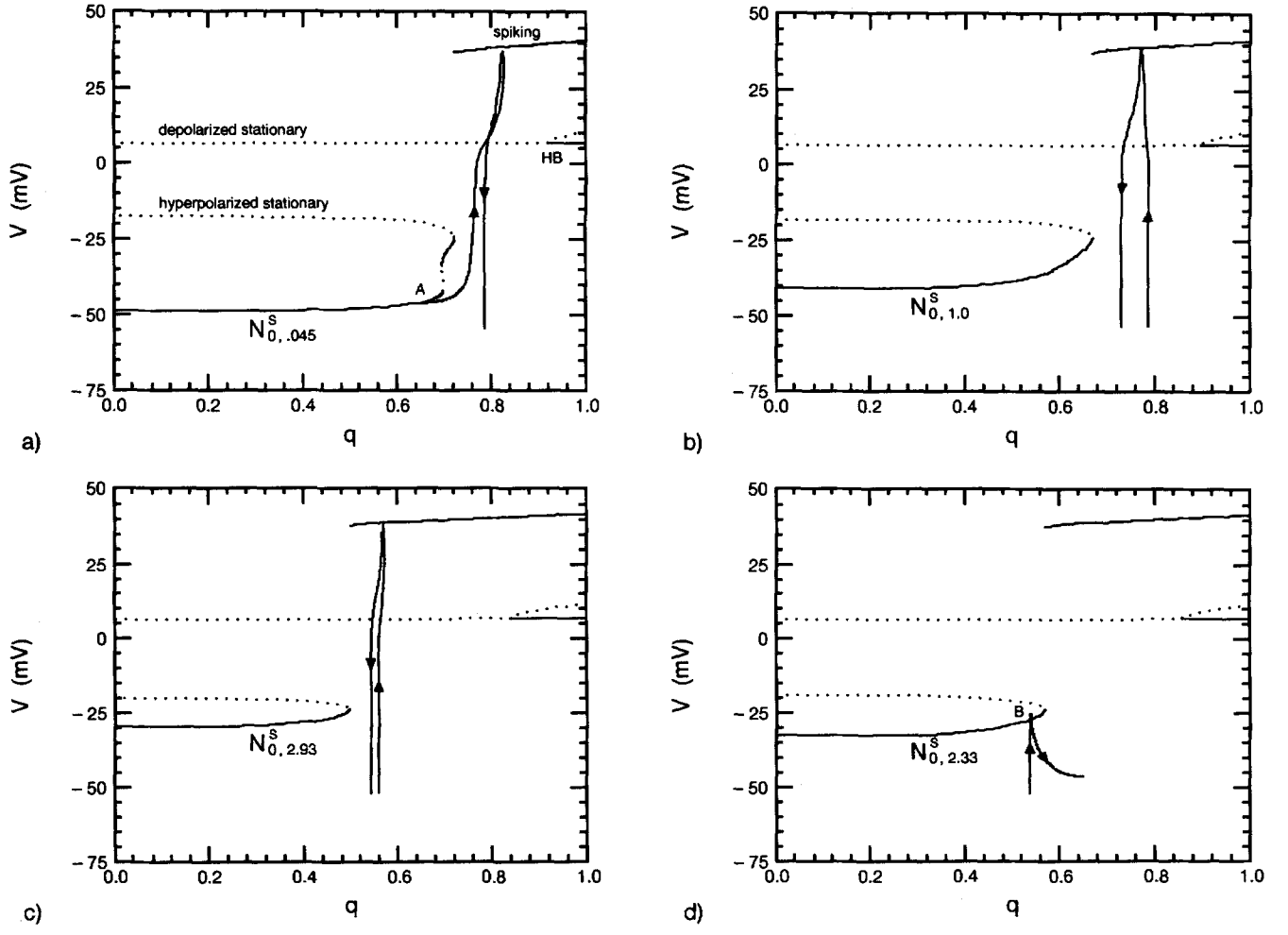

Fig. 2a–d. Dissection of the control ($S = 0$) bursting oscillation. Reduced-system stationary and periodic spiking branches are shown along with portions of the full-system orbit (directed curves) projected onto the $q - V$ plane. Periodic solutions are represented by the maximum voltage over an oscillation. *Solid curves* represent stable solutions, while *dashed curves* represent unstable solutions. **a** $z = 0.045$ nA; **b** $z = 1.0$ nA; **c** $z = 2.93$ nA; **d** $z = 2.33$ nA

hyperpolarized stable stationary solution of (12) coalesces with an unstable stationary solution. The phase point moves beyond this saddle node, after which it is attracted to the reduced-system spiking attractor. In this way the passive phase is ended and the active phase begun.

After the first spike, at $V = -25$ mV in the ascending phase of the second spike, $z \approx 1.0$ nA. The reduced-system solution branches at this value of z, along with the projection onto the $q - V$ phase plane of the second spike generated by (11), are displayed in Fig. 2b. With the increase in z the hyperpolarized stationary branch has deformed and moved to the left. The value of q during the ascending phase of the spike is approximately 0.8, and since the only attractor existing at this value of q is the spiking attractor, the entire second spike will be generated. Notice, however, that the phase point moves to the left during the descending phase of the spike, thus travelling in the same direction as the stationary solution branch.

At $V = -25$ mV in the ascending phase of the eighth spike, $z \approx 2.93$ nA. The stationary solution branch has continued to narrow and move to the left, as has the projection of the eighth spike (Fig. 2c). Again, since the orbit does not intersect $N^S_{0,2.93}$ in the ascending phase, the complete spike is generated.

At $V = -25$ mV in the ascending phase of the tenth spike, z has decreased to approximately 2.33 nA. This decrease occurs because the increase of z with each spike is exceeded by the exponential decrease of z between spikes at this late stage in the burst. As we see from Fig. 2d, the full system orbit has now "caught up with" the reduced stationary branch and the two intersect at location B. Thus, the orbit is attracted to a point on the stationary branch and the tenth spike is terminated prematurely, with voltage decaying after rising to approximately -25 mV. In this way the system passes from the active to the passive phase of the oscillation.

The rise and premature termination of the spike shown in Fig. 2d is the rising phase of the DAP. The falling phase, along with the rest of the interburst, is dissected in Fig. 3. At location B, $z \approx 2.33$ nA and the phase point lies close to $N^S_{0,2.33}$, having been captured by a point on this attracting branch. Since the system is no longer spiking, z decays and at location C has fallen to approximately 1.0 nA. By location D the falling phase of the DAP is complete, as z has decreased to 0.045 nA $\approx z_\infty$. It is evident that the phase point is following the reduced-system stationary curves down and to the right as they deform with the decrease in z. From location D the phase point travels along $N^S_{0,0.045}$ until its point of termination, at which time the phase point leaves the branch and is attracted once again to the spiking attractor, reinitiating the active phase.

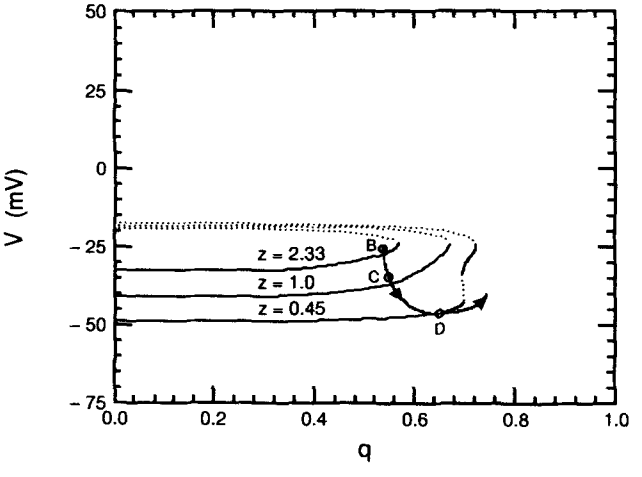

Fig. 3. Falling phase of the DAP and the remainder of the interburst. At locations B, C, D on the full-system orbit $z = 2.33$ nA, 1.0 nA and 0.045 nA respectively

The reduced-system depolarized stationary branch and the periodic spiking branch (Fig. 2) will now be described. The latter bifurcates branches off the former via a Hopf bifurcation. Otherwise, the depolarized stationary branch plays no clear role in the system dynamics. The spiking branch is unstable upon its emergence, but gains stability through a saddle-node bifurcation and a pair of period-doubling bifurcations. These bifurcations occur outside the physical range of q and are not illustrated. For $q \leqslant 1$ the branch keeps its stability until its termination via an infinite-period homoclinic bifurcation. That is, if q_H denotes the value of q at which the rightmost saddle-node bifurcation occurs on the hyperpolarized stationary branch for some fixed z, then as the spiking branch is traversed the period of the reduced-system oscillation grows without bound as $q \to q_H$. This rightmost limit point is thus a homoclinic point of (12).

3.2 Reduced-system analysis of the modulatory effects of serotonin

The effects of 5-HT on the model bursting oscillation are shown in Fig. 9 of Bertram (1993). At low concentrations the depth and duration of the interburst are increased, as is the number of spikes in the active phase. At higher concentrations spiking is terminated and the cell remains silent at a hyperpolarized voltage. At even higher concentrations the cell spikes tonically. Thus, 5-HT has both inhibitory and excitatory effects when applied to the same neuron, contrary to what is typically expected of a neurotransmitter. These effects are perhaps best understood in terms of alterations made to the solution structure of the reduced system (12). Separate analysis is carried out below for low concentrations and medium to high concentrations of applied 5-HT.

3.2.1 Low concentrations of serotonin

In Fig. 4 hyperpolarized stationary solution branches to (12) are shown for several values of z taken on during the passive phase of the bursting oscillation. S is set to 0.3, representing a low concentration of 5-HT. Superimposed is the projected orbit of the full system during the interburst. The orbit initially rises to form a spike, but is stopped prematurely due to attraction to a stable point

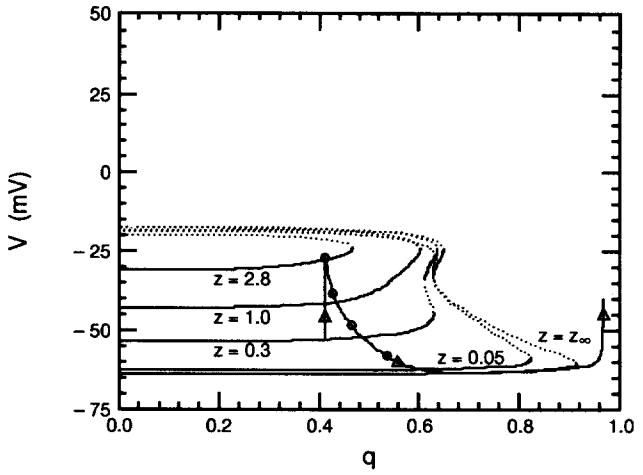

Fig. 4. Reduced-system hyperpolarized stationary branches for $S = 0.3$. Also projected onto the $q - V$ plane is the slow manifold ($z = z_\infty$) and the orbit of the full system during the interburst (directed curve). Marked points indicate locations on the orbit at which $z = 2.8$ nA, 1.0 nA, 0.3 nA and 0.05 nA

on the $z = 2.8$ nA branch [i.e. $N^S_{3,2.8}$ (0.412), the point on $N^S_{3,2.8}$ at which $q = 0.412$]. From here the phase point follows the reduced-system stationary curves down and to the right as voltage decreases and q approaches its steady-state value. Eventually the system reaches a pseudo-equilibrium state at which all variables other than q have reached equilibrium. The collection of these states for all applicable values of q forms a one-dimensional "slow manifold" along which the orbit travels after completion of the DAP. The slow manifold is traversed until its termination via saddle-node bifurcation, after which the phase point is again attracted to the spiking solution and the active phase reinitiated.

The projection of the slow manifold onto the $q - V$ plane is labelled "$z = z_\infty$" in Fig. 4, where $z_\infty = \tau_z k_z m^3_\infty(V_\infty) h_\infty(V_\infty)$ and where V_∞ is a function of q. The lower knee of the manifold, as well as the lower knee of stationary branches corresponding to z near z_∞, is greatly exaggerated with respect to the lower knee of any of the branches in Fig. 3, both in extent and depth. Since the phase point travels along this exaggerated manifold during the latter part of the passive phase, both the depth and duration of the interburst will be greater for the $S = 0.3$ oscillation than for the control oscillation. The effects of 5-HT on the interburst are, therefore, due exclusively to this exaggeration of the lower knee of the reduced-system stationary branches.

The other effect of low concentrations of 5-HT, the increase in the number of spikes per burst, is again largely a consequence of the exaggeration of the lower knee of the slow manifold, which places the phase point further to the right in the $q - V$ plane at the initiation of the active phase. An additional factor is the deformation of the upper knee (which, for some z, is the only knee) of the family of stationary branches. At any value of z, the location of the upper knee is further to the left when $S = 0.3$ than at control. This is because, with the increase in $\bar{g}_{NSR}$, q must reach a lower value before I_{NSR} will become sufficiently small for the spiking to be terminated. As a result of these two factors, more spikes are generated as more of the spiking branch must be traversed during the active phase.

3.2.2 Medium to high concentrations of serotonin

As S is increased, the lower knee of the slow manifold moves to the right in the $q - V$ plane, until at $S = S_1 = 0.305$ the knee intersects the projection of the curve C_1 at $q = q_\infty = 0.990$. This latter curve is the intersection of nine nullclines, excluding the V nullcline, and is parameterized by V. The intersection of the slow manifold with C_1 is located at the point of intersection of the ten nullclines of the full system, and thus is a stationary solution of (11). As S is increased beyond S_1 the two curves intersect at two hyperpolarized locations rather than one, so the single hyperpolarized stationary solution splits into an unstable and a stable solution. The slow manifold and C_1 also intersect at a depolarized location for each S, corresponding to an unstable solution of (11). For the asymptotic stationary solution structure of the full system, see Fig. 10 in Bertram (1993).

With the birth of the stationary solution at S_1 the bursting oscillation is replaced for all larger values of S by a stable stationary solution coexisting with a stable beating solution. Poincaré sections are employed to investigate this region of bistability. A Poincaré section is constructed for the control bursting oscillation by sampling the oscillation (after the removal of transients) at $V = -25$ mV in the ascending phase of each action potential (as well as the DAP), recording both z and q. This data is plotted in the $z - q$ plane in Fig. 5a. Along with the Poincaré section, a curve is included which is a graph of the q value of the upper knee of the reduced-system stationary branch for each value z at which it exists. That is, the curve is a branch of limit points which tells us, for instance, that as z increases, q decreases, so that the location of the upper knee moves to the left in the $q - V$ plane as z increases during the first portion of the burst (compare with Fig. 2). The curve is also a branch of homoclinic points since, when $S = 0$, the upper knee is to the right of the lower knee in the $q - V$ plane for each z at which the lower knee exists. For z sufficiently large, the upper knee ceases to exist, in which case no hyperpolarized stationary solution of (12) exists for any value of q.

The location of the upper knee is important, since, as was observed in Fig. 2, a burst terminates when the orbit falls to the left of the upper knee in the $q - V$ plane. In the $z - q$ plane, this corresponds to the orbit falling below the upper-knee limit point (LP) branch. At control, there are nine spikes in the burst and one DAP. The spikes correspond to the Poincaré points above the LP branch in Fig. 5a, while the DAP corresponds to the single point below the LP branch. From the location of this latter point, the orbit (not shown) is directed up and to the left until the leftmost Poincaré point is reached and the spiking resumed.

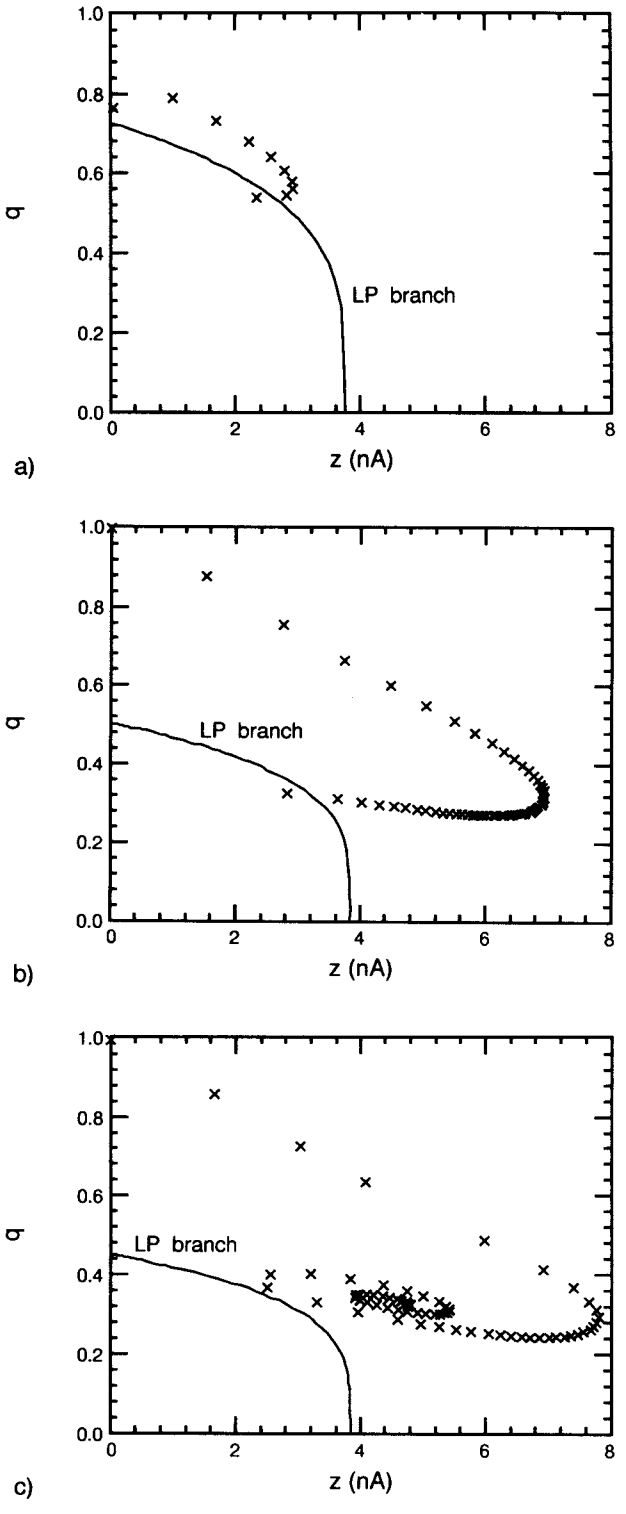

Fig. 5. Poincaré section and upper-knee limit point (*LP*) branch for **a** $S = 0$, **b** $S = 0.5$, and **c** $S = 0.65$. The Poincaré section (each point marked with an "×") is constructed by sampling at $V = -25$ mV in the ascending phase of the action potential or DAP

At $S = 0.5$, at which the system does not burst, the corresponding Poincaré section and LP branch are shown in Fig. 5b. Here a suprathreshold voltage perturbation has been applied to the resting equilibrium system, producing a long transient burst of action potentials. The point in the upper-left corner of the figure corresponds to the first spike following the perturbation, while the point below the LP branch corresponds to the DAP which follows the transient burst. From this latter point the orbit (not shown) moves up and to the left until the stable equilibrium point is reached. The location of this point in the $z - q$ plane ($z = 5.23 \times 10^{-4}$ nA, $q = 0.995$) is above the LP branch, yet the system does not reenter the active phase. This is not surprising, since the location of the upper knee is important only in the passage from the active to the passive phase. It is the lower knee which is important in the passage from the passive to the active phase.

A similar voltage perturbation is applied to the resting system with $S = 0.65$ (Fig. 5c). This time no Poincaré point crosses the LP branch, and the spiking never terminates. Instead, the sequence of Poincaré points approaches a stable fixed point above the LP branch, corresponding to a beating oscillation.

Due to the all-or-nothing nature of the action potential, if a voltage perturbation is applied to the resting system of magnitude sufficient to induce a spike, the precise magnitude of the perturbation is unimportant. In other words, all suprathreshold voltage perturbations have the same effect on the system. With this consideration, we see evidence in Fig. 5 that it is not possible to reach the basin of attraction of the beating oscillation by applying a voltage perturbation to the stationary solution when "medium" concentrations of 5-HT ($S_1 < S < S_3$, where $S_3 \approx 0.65$) have previously been applied. However, any suprathreshold voltage perturbation is sufficient to move the system off the stationary point and into the beating basin after previous application of a "high" concentration ($S_3 \leqslant S \leqslant 1.0$) of 5-HT. Therefore, at medium 5-HT concentrations the neuron will generally be observed in the silent state, while for larger concentrations it will often be found in the beating state.

As was mentioned earlier, when $S = 0$ and for any z, the rightmost limit point of the reduced-system hyperpolarized stationary branch is a homoclinic point for the system (12). For most $S > 0$, however, the lower knee extends beyond the upper knee for a range of values of z, in which case the upper-knee limit point is not a homoclinic point. However, neither is the lower-knee limit point a homoclinic point. This is demonstrated in Fig. 6, where the hyperpolarized stationary branch is plotted for $S = 0.3$, $z = 0.05$ nA along with the minimum voltage of the spiking oscillation for each value q at which the oscillation exists. The oscillation clearly exists at values of q to the left of the lower knee, finally terminating at a homoclinic point located on the stationary branch between the lower knee and the "switchback" limit point separating the lower and upper knee.

In Fig. 7a the upper-knee, lower-knee, and switchback LP branches are illustrated for $S = 0.3$. Superimposed is the Poincaré section of the active phase of the periodic burst and the projection onto the z – q plane of the orbit during the interburst. Notice that the lower-knee and switchback limit points coalesce at $z \approx 0.5$ nA, $q \approx 0.6$, so that only one knee exists for all larger values

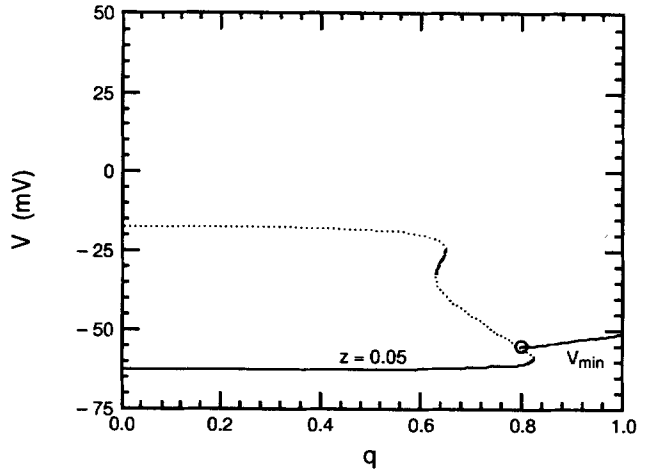

Fig. 6. Reduced-sytem hyperpolarized stationary branch for $S = 0.3$, $z = 0.05$ nA. Also, minimum voltage of the spiking oscillation for all q for which it exists. The homoclinic point is indicated by "○"

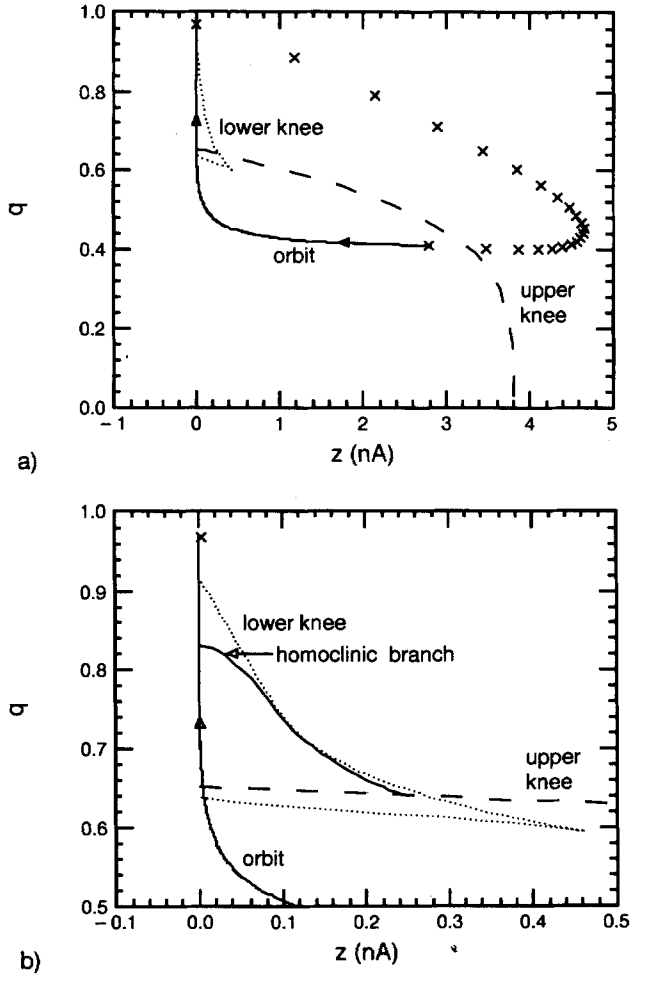

Fig. 7a, b. Analysis of the $S = 0.3$ bursting oscillation. **a** . . . , Lower-knee and switchback branch; – –, upper-knee branch; × × ×, Poincaré section; directed curve, projection of interburst orbit. **b** . . . , Lower-knee and switchback branch; – –, upper-knee branch; —, homoclinic branch; ×, Poincaré point; directed curve, projection of interburst orbit

of z. When a Poincaré point crosses the upper-knee branch the active phase is terminated. Because the upper knee is a homoclinic point at this location in the $z - q$ plane, the spikes of the active phase are generated at a relatively low frequency near this point of termination. During the DAP the orbit travels almost horizontally in the $z - q$ plane as I_D, and thus z, discharges. Following the DAP, $z \approx z_\infty$ so that the orbit travels almost vertically in the $z - q$ plane as I_{NSR} loses its inactivation. The passive phase is terminated when the orbit crosses the lower-knee branch and a new spike is generated. For $S_1 < S$, the orbit reaches an equilibrium point before the lower-knee branch is crossed and the active phase is not reentered.

The portion of Fig. 7a containing the lower-knee branch is enlarged in Fig. 7b. The upper-knee branch consists of homoclinic points up until the point at which the lower knee extends beyond the upper knee in the $q - V$ plane. The homoclinic points from this point on are included in Fig. 7b. Because of the close proximity of the first few Poincaré points to the homoclinic branch, the first few spikes of the active phase are generated with low frequency.

4 Sensitivity to synaptic perturbations

4.1 Passive-phase perturbations

How does 5-HT affect the sensitivity? This question was briefly addressed above and will be investigated here in more detail, beginning with the effects of perturbations applied during the passive phase of the bursting oscillation and, when $S > S_1$, to perturbations applied to the resting system. The reduced system of equations will again be employed and instantaneous depolarizing voltage perturbations applied as an approximation to excitatory synaptic events.

At each value of z during the passive phase of the control oscillation the reduced-system stationary branch has at least one stable component, $N^S_{0,z}$, and one unstable component, $N^u_{0,z}$ (Fig. 3). At any such z and at any value of q taken on during the passive phase, the point $N^S_{0,z}(q)$ draws the full-system orbit to it, while $N^u_{0,z}(q)$ repels the orbit. If a depolarizing voltage perturbation is applied to the orbit of sufficient magnitude to displace the phase point to a location above $N^u_{0,z}(q)$, then at least one spike is generated, terminating the passive phase. The later in the interburst the perturbation is applied, the greater the number of spikes which will be generated as a result of the perturbation. This is consistent with experimental data (Benson and Adams 1987). However, at all times during the interburst, particularly in the post-DAP interburst, the threshold $N^u_{0,z}(q)$ is at a voltage significantly higher than the voltage of the phase point, so that only large perturbations can terminate the passive phase and, in effect, reset the phase of oscillation. This has also been observed experimentally (Carpenter et al. 1978).

Because 5-HT exaggerates the lower knee of the family of stationary branches, it lowers the spike threshold

during the post-DAP interburst (Fig. 4). Therefore, while large perturbations are still required to terminate the passive phase when applied during the DAP, much smaller perturbations suffice when applied after the DAP. In this way, the application of 5-HT increases the sensitivity of the neuron to excitatory synaptic perturbations applied during the passive phase.

We now turn to an examination of perturbations applied to the system at rest. In Fig. 8 a portion of the slow manifold is shown for the case $S = 0.65$. Also shown is the curve C_1, which was described earlier for the case $S = 0$. Any point of intersection of this curve with the slow manifold corresponds to a point of intersection of all ten nullclines, and hence to a stationary solution of the full system (11). Two such points exist at hyperpolarized voltages. The lower point of intersection, at $N^S_{0.65,z_\infty}(q_\infty)$, is the single stable solution, while the intersection at $N^u_{0.65,z_\infty}(q_\infty)$ is an unstable solution [an additional unstable solution of (11) occurs where the curve C_1 intersects the reduced-system depolarized stationary branch]. Note that $q_\infty \approx 0.992$ at the stable point of intersection, while $q_\infty \approx 0.936$ at the unstable point.

If a voltage perturbation is applied at $N^S_{0.65,z_\infty}(q_\infty)$ of sufficient magnitude to displace the phase point above the $N^u_{0.65,z_\infty}$ curve [more precisely, across the stable manifold of the point in eight-dimensional space whose projection onto the $q - V$ plane is on $N^u_{0.65,z_\infty}$ directly above $N^S_{0.65,z_\infty}(q_\infty)$], then a spike will be generated and the system will continue to spike as the orbit approaches the stable beating solution (see Fig. 5c). A similar scenario occurs for lower values of S, although the perturbation-induced spiking is transient in such cases (Fig. 5b). Hence, the point on $N^u_{0.65,z_\infty}$ directly above $N^S_{0.65,z_\infty}(q_\infty)$ is a threshold point, lying close to the invariant manifold (or separatrix) through $N^u_{0.65,z_\infty}(q_\infty)$ which separates the stationary basin of attraction and the beating basin of the full system.

4.2 *Active-phase perturbations*

The effects of voltage perturbations applied during the active phase of a bursting oscillation or during a beating oscillation are investigated next. Analysis is made in the $z - q$ plane with the aid of a Poincaré section of the oscillation and the appropriate upper-knee LP branch. Inhibitory synaptic events are simulated by perturbing the membrane potential at -25 mV in the ascending phase of the action potential to a more negative voltage. Phase plane analysis (not shown) indicates that perturbations applied in such a manner are among the most successful in prematurely terminating the active phase of the burst.

In Fig. 9 perturbations are applied to various spikes in the active phase of the control bursting oscillation. In each case, the membrane potential is perturbed from -25 mV to -35 mV. The spike to which the perturbation is applied is terminated prematurely, so that z continues to decay exponentially without being recharged. As a result, the orbit initially moves to the left in the $z - q$ plane before switching directions as a new spike finally develops. The initial leftward segment of the orbit following a perturbation is plotted in Fig. 9, emanating from the appropriate Poincaré point. If the perturbation is applied to the ascending phase of spike 2 there is little subsequent leftward movement in the orbit, since z is small early in the burst and thus the exponential decay in z following the perturbation is small. In contrast, if the perturbation is applied in the ascending phase of spike 8, then the orbit will be displaced far to the left in the $z - q$ plane. In fact, the phase point is displaced across the LP branch and the active phase terminated without any additional spikes.

This analysis reveals a couple of points. First, perturbations applied early in the active phase of the burst

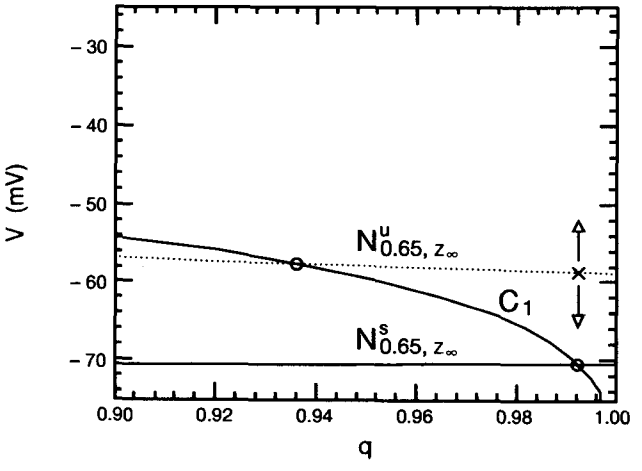

Fig. 8. Portion of the slow manifold projection along with the projection of the curve C_1, for $S = 0.65$. Full-system stationary points are located at the intersections of these curves ("○"). The point ("×") on $N^u_{0.65,z_\infty}$ directly above the stable stationary point is a threshold point

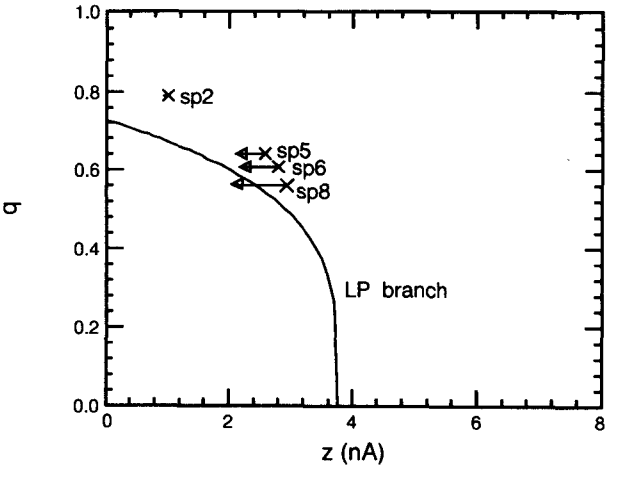

Fig. 9. The immediate effect of hyperpolarizing voltage perturbations applied to various spikes in the active phase of the control bursting oscillation. Four trials are carried out, the perturbation being applied in the ascending phase of a different spike (labeled) in each trial. The directed line segment emanating from each Poincaré point is the leftward portion of the orbit following the perturbation

must be very large to terminate this phase. Indeed, it is not even possible to terminate the active phase with hyperpolarizing perturbations applied during the first few spikes, since the LP branch does not exist to the left of the corresponding Poincaré points. Later in the burst, much smaller perturbations are sufficient to prematurally terminate the active phase. One may also conclude from this analysis that upon the application of 5-HT the system becomes less sensitive to perturbations applied during the active phase. This is because the Poincaré points of the serotonin-modulated system lie further from the LP branch than do those for the control system (see, for example, Fig. 5c).

If a hyperpolarizing perturbation is applied to a beating oscillation (represented by a single point in the Poincaré section), the oscillation will be terminated and the system will approach its stationary equilibrium as long as the perturbation is large enough so that the perturbed orbit crosses the LP curve. Otherwise, the beating oscillation will persist.

5 Summary and discussion

In this paper the endogenous bursting oscillation generated in the somal region of molluscan neuron R_{15} is dissected using a mathematical model consisting of a system of ten coupled nonlinear ordinary differential equations. Using tools from dynamical systems theory, along with a reduced system of equations formed from the original system by treating two variables as slowly varying parameters, the bursting oscillation is shown to be generated as the fast subsystem sweeps back and forth between spiking attractors and stationary attractors with variation of the two slow variables. This analysis reveals that the control system is relatively insensitive to synaptic voltage perturbations applied during the passive phase. In addition, we see that suprathreshold perturbations applied later in the passive phase induces an active response consisting of more spikes than one applied early in the passive phase. Both of these observations are consistent with experimental data (Benson and Adams 1987; Carpenter et al. 1978). Finally, we see that perturbations applied later in the active phase are more likely to terminate the spiking than those applied early in the active phase.

When the neurotransmitter serotonin is applied exogenously to neuron R_{15} it modulates the endogenous voltage waveform in a manner which is somewhat uncharacteristic of neurotransmitters. This waveform modulation is investigated and the dynamics behind the modulation illuminated using the same tools employed in the analysis of the control oscillation. This analysis indicates that the application of serotonin makes the neuron more sensitive to synaptic perturbations applied during the passive phase of bursting as the spike threshold is lowered during the post-DAP interburst. Serotonin also makes the system less sensitive to perturbations applied during the active phase, with perturbations applied later in the active phase again being more effective than those applied early in prematurally terminating the active phase.

With sufficiently large applications of serotonin the bursting oscillation may be terminated and the system found in a quiescent state, or the oscillation may be transformed into a continuous spiking or beating oscillation. These qualitative changes in waveform are analyzed and recast in terms of competition between a stationary and a beating attractor. A voltage threshold is found above which perturbations from the resting state will lead to either a transient burst of spikes or a continuous train of spikes. Additionally, a condition is given which must be satisfied in order for a hyperpolarizing voltage perturbation to perturb the system from its beating attractor to its stationary attractor.

These results should be interpreted in light of the role played by R_{15} in regulating water balance in *Aplysia*. R_{15} is a neuroendocrine cell which releases, with each voltage spike, a hormone which induces the intake of salt and water through the skin of the animal. By increasing the sensitivity of the neuron to excitatory synaptic perturbations applied during the passive phase of the bursting oscillation or to the neuron in its quiescent state, serotonin increases the ability of neurons synapsing onto R_{15} to increase salt and water intake, thus strengthening the coupling between the electrical activity of surrounding neurons and water balance in the animal. Since serotonin mimics the effects on R_{15} of egg-laying hormone, which is secreted by a pair of neuroendocrine cell clusters known as *bag cells* for up to 40 min during egg laying (Kandel 1979; Mayeri et al. 1985; Levitan et al. 1987), the modulations in voltage waveform and system sensitivity can be expected to persist throughout the egg-laying process.

Acknowledgements. The author would like to thank the members of the Mathematical Research Branch at the National Institute of Diabetes and Digestive and Kidney Diseases for discussions which led to further analysis of the homoclinic structure of the reduced system. This work was supported by the Florida State University Supercomputer Computations Research Institute, which is partially funded by the US Department of Energy through contract no. DE-FC05-85ER250000.

Appendix: The model R_{15} system

The voltage equation is

$$\frac{dV}{dt} = -(I_{spike} + I_{sub} - I_{app})/C_M$$

where

$$I_{spike} = I_{Na} + I_{Ca} + I_{K1} + I_{K2} + I_L,$$

$$I_{sub} = I_{NSR} + I_D + I_R$$

and

$$I_{Na} = \bar{g}_{Na} m^3 h (V - V_{Na}), \quad I_{Ca} = \bar{g}_{Ca} x^2 (V - V_{Ca})$$

$$I_{K1} = \bar{g}_{K1} n^2 j (V - V_K), \quad I_{K2} = \bar{g}_{K2} (V - V_K)/(\mu + 1)$$

$$I_L = g_L (V - V_L), \quad I_{NSR} = \bar{G}_{NSR} q^4 y_\infty(V)(V - V_{Ca})$$

$$I_D = -z, \quad I_R = \bar{G}_R r_\infty(V)(V - V_K).$$

Other variables change with time according to

$$\frac{dm}{dt} = [m_\infty(V) - m]/\tau_m(V), \qquad \frac{dn}{dt} = [n_\infty(V) - n]/\tau_n(V)$$

$$\frac{dh}{dt} = [h_\infty(V) - h]/\tau_h(V), \qquad \frac{dj}{dt} = [j_\infty(V) - j]/\tau_j(V)$$

$$\frac{dx}{dt} = [x_\infty(V) - x]/\tau_x(V), \qquad \frac{d\mu}{dt} = [\mu_\infty(V) - \mu]/\tau_\mu$$

$$\frac{dq}{dt} = [q_\infty(c) - q]/\tau_q(V), \qquad \frac{dz}{dt} = k_z m^3 h - z/\tau_z$$

$$\frac{dc}{dt} = -k_i[I_{Ca} + I_{NSR}] - k_e c$$

All parameter values, infinity functions and time constants are given in Bertram (1993), as are expressions for $\bar{G}_{NSR}(S)$ and $\bar{G}_R(S)$.

References

Atwater I, Dawson M, Scott A, Eddlestone G, Rojas E (1980) The nature of the oscillatory behavior in electrical activity for the pancreatic β cell. In: Georg Thieme (ed) Biochemistry and biophysics of the pancreatic β-cell. Verlag, New York, pp 100–107

Benson JA, Adams WB (1987) The control of rhythmic neuronal firing. In: Kaczmarek LK, Levitan IB (eds) Neuromodulation: the biochemical control of neuronal excitability. Oxford University Press, New York, pp 100–118

Benson JA, Levitan IB (1983) Serotonin increases an anomalously rectifying K^+ current in the *Aplysia* neuron R_{15}. Proc Natl Acad Sci USA 80:3522-3525

Bertram R (1993) A computational study of the effects of serotonin on a molluscan burster neuron. Biol Cybern 69: 257–267

Canavier C, Clark JW, Byrne JH (1991) Simulation of the bursting activity of neuron R_{15} in *Aplysia*: role of ionic currents, calcium balance and modulatory transmitters. J Neurophysiol 66(6):2107–2124

Carpenter DO, McCreery MJ, Woodbury CM, Yarowsky PJ (1978) Modulation of endogenous discharge in neuron R_{15} through specific receptors for several transmitters. In: Chalazonitis N, Boisson M (eds) Abnormal neuronal discharges. Raven, New York, pp 189–203

Chay TR, Rinzel J (1985) Bursting, beating, and chaos in an excitable membrane model. Biophys J 47:357–366

Decroly O, Goldbeter A (1987) From simple to complex oscillatory behaviour: analysis of bursting in a multiply regulated biochemical system. J Theor Biol 124:219–250

Doedel EJ (1981) AUTO: a program for the automatic bifurcation and analysis of autonomous systems. Cong Num 30:265–284

Drummond AH, Benson JA, Levitan IB (1980) Serotonin-induced hyperpolarization of an identified *Aplysia* neuron is mediated by cyclic AMP. Proc Natl Acad Sci USA 77:5013–5017

Eckert R, Lux HD (1976) A voltage-sensitive persistent calcium conductance in the neuronal somata of *Helix*. J Physiol 254:129–151

Kandel ER (1979) Behavioral biology of *Aplysia*. Freeman, San Francisco, p 324

Kramer RH, Zucker RS (1985a) Calcium-dependent inward current in *Aplysia* bursting pace-maker neurones. J Physiol 362:107–130

Kramer RH, Zucker RS (1985b) Calcium-induced inactivation of calcium current causes the inter-burst hyperpolarization of *Aplysia* bursting neurones. J Physiol 362:131–160

Levitan ES, Kramer RH, Levitan IB (1987) Augmentation of bursting pace-maker activity by egg-laying hormone in *Aplysia* neuron R_{15} is mediated by a cyclic AMP-dependent increase in Ca^{2+} and K^+ currents. Proc Natl Acad Sci USA 84:6307–6311

Levitan ES, Levitan IB (1988) Serotonin acting via cyclic AMP enhances both the hyperpolarizing and depolarizing phases of bursting pacemaker activity in the *Aplysia* neuron R_{15}. J Neurosci 8:1152–1161

Lotshaw DP, Levitan ES, Levitan IB (1986) Fine tuning of neuronal electrical activity: modulation of several ion channels by intracellular messengers in a single identified nerve cell. J Exp Biol 124:307–322

Mayeri E, Rothman BS, Brownell PH, Branton WD, Padgett L (1985) Nonsynaptic characteristics of neurotransmission mediated by egg-laying hormone in the abdominal ganglion of *Aplysia*. J Neurosci 5:2060–2077

Plant RE (1978) The effects of calcium^{++} on bursting neurons. Biophys J 21:217–237

Plant RE, Kim M (1975) On the mechanism underlying bursting in the *Aplysia* abdominal ganglion R_{15} cell. Math Biosci 26:357–375

Rinzel J, Lee YS (1987) Dissection of a model for neuronal parabolic bursting. J Math Biol 25:653–675

Rorsman P, Trube G (1986) Calcium and delayed potassium currents in mouse pancreatic β-cells under voltage clamp conditions. J Physiol 375:531–550